UNIVERSITY OF CALIFORNIA SAN DIEGO

Tau isoforms promote differences in transposable element activation, gene expression and cell dysfunction

A thesis submitted in partial satisfaction of the requirements for the degree Master of Science

in

Biology

by

Jennifer Grundman

Committee in charge:

Professor Robert A. Rissman, Chair
Professor Randolph Hampton, Co-Chair
Professor Roberto Malinow

2020

The thesis of Jennifer Grundman is approved, and it is acceptable in quality and form for publication on microfilm and electronically:

_____

_____

Co-Chair

_____

Chair

University of California San Diego

2020

TABLE OF CONTENTS

ACKNOWLEDGEMENTS

I would like to thank Dr. Robert Rissman, the Chair of my committee, for his guidance and words of encouragement throughout this work. I am truly grateful for the opportunities he has given me to contribute to his lab and to explore my interests during this project.

I would also like to express my gratitude to Dr. Brian Spencer for his thoughtful mentorship and patience. His support proved invaluable throughout this project. Furthermore, I would like to thank him for providing the lentiviruses needed to conduct this project.

My gratitude is also extended to Floyd Sarsoza for assisting in running the Western blots needed to validate the viral constructs.

This thesis is currently being prepared for submission for publication of the material. Grundman, J., Spencer, B., Sarsoza, F., Rissman, R.A. The dissertation/thesis author was the primary investigator and author of this material.

ABSTRACT OF THE THESIS

Tau isoforms promote differences in transposable element activation, gene expression and cell dysfunction

by

Jennifer Grundman

Master of Science in Biology

University of California San Diego, 2020

Professor Robert A. Rissman, Chair
Professor Randolph Hampton, Co-Chair

Alternative splicing of the gene MAPT produces several isoforms of tau protein; the overexpression of these isoforms is characteristic of tauopathies, which are

untreatable neurodegenerative diseases. Though non-canonical functions of tau have begun to draw interest, tau isoforms' role in these phenomena has not been examined and may reveal new details of tau-driven pathology. In particular, tau has been shown to promote activation of transposable elements, which are highly regulated nucleotide sequences that replicate throughout the genome and are thought to promote immunologic responses and cellular stress. In this study, we utilized differentiated SH-SY5Y cells infected with lentiviral constructs of tau isoforms and treated with beta-amyloid oligomers, along with publicly available RNA-sequencing data from human samples, to address tau isoforms' roles in promoting cell damage and dysregulation of genes and transposable elements at a locus-specific level. Our analyses reveal that overexpression of different tau isoforms and their interactions with beta-amyloid in SH-SY5Y cells result in isoform-specific changes in the transcriptome, with tau isoforms showing locus-specific transposable element dysregulation patterns that parallel those seen in patients with Alzheimer's disease and progressive supranuclear palsy. We also demonstrated differences in rates of cell death in SH-SY5Y cells infected with lentiviruses of different tau isoforms Transposable element expression at the locus-level showed increased dysregulation of L1 and Alu sites, which are thought to be drivers of pathology in other neurological diseases. These results demonstrate the importance of examining tau isoforms' roles in neurodegeneration and bolster support for further examining transposable element dysregulation in tauopathies.

Introduction

Tauopathies form a class of widespread neurodegenerative diseases for which there are currently no ameliorative or curative treatments. Though tauopathies are broadly characterized by pathological tau protein, the exact expression of the protein varies considerably across diseases, with some labeled “primary tauopathies,” in which tau is the main pathological feature and with some labeled “secondary tauopathies,” in which abnormal tau expression coexists with other pathologies or may not be considered the primary pathologic feature (Lebouvier et al., 2017). Tau protein itself comes in six separate isoforms formed from the alternative splicing of the gene MAPT, located on chromosome 17. These isoforms are categorized by their number of N-terminal repeats (0, 1, or 2) and the number of their microtubule-binding repeats (3 or 4; these are respectively referred to as 3R or 4R tau isoforms) (Guo et al., 2017).

Tau isoform imbalance, posttranslational modifications, and abnormal aggregation are frequent suspects in the etiology of many phenotypically distinct neurodegenerative diseases, such as Alzheimer’s disease (AD), progressive supranuclear palsy (PSP), Pick’s disease (PiD), and chronic traumatic encephalopathy (Lebouvier et al., 2017). Despite this, little research has been done to isolate the unique roles of tau isoforms in neurodegenerative processes. While these isoforms may overlap in their functions, recent studies present evidence that imbalances in them can lead to different impairments. For instance, 3R and 4R tau isoforms have been shown to respectively regulate anterograde and retrograde axonal transport of amyloid precursor protein, a process that is disrupted when one of these isoforms becomes overexpressed

(Lacovich et al., 2017). Other studies present evidence of interaction between tau isoforms by mediating each other's aggregation or of greater toxicity of one type of isoform over another (Adams et al., 2010; Sealey et al., 2017). Thus the treatment of tau as one pathological protein instead of as a collection of isoforms with unique functions could mask important insights into the pathogenesis of tauopathies. As these diseases are widely prevalent and currently have no curative or therapeutic treatments, understanding the exact mechanisms underlying their pathology are critical.

Most tau research in the context of neurodegeneration has focused on its stabilization of microtubules in the cytoplasm and axons (Sotiropoulos et al., 2017). In these areas, its abnormal expression and aggregation into intracellular neurofibrillary tangles (NFTs) is suspected to destabilize the cell and hinder cell processes, eventually resulting in cell death (Guo et al., 2017). However, it has become apparent in recent years that tau has significant non-canonical roles in other critical cell functions that are affected in neurodegeneration (Sotiropoulos et al., 2017). Recent studies into nuclear tau, for instance, present evidence that tau not only binds to DNA and RNA, but may have a protective role against heat stress (Guo et al., 2017; Sultan et al., 2011; Violet et al., 2014). Moreover, dysfunction of tau has been linked to heterochromatin relaxation, epigenetic and transcriptomic changes, and disruption of normal protein synthesis patterns (Frost et al., 2014; Klein et al., 2019; Meier et al., 2016).

Tau-influenced epigenetic and transcriptomic changes may help account for increased transposable element (TE) expression seen in some tauopathies. Two recent studies have found that tau expression correlates with expression TEs in diseases such as AD and PSP (Guo et al., 2018; Sun et al., 2018). TEs are nucleotide sequences that

are able to relocate throughout the genome, with the potential to cause insertion mutations, carry out regulatory functions, and promote inflammation through causing increased interferon responses (Tam et al., 2019). Generally speaking, TEs are separated into two distinct classes based on their method of transposition. DNA transposons rely on transposases to recognize two bordering repeat sequences, which allow the transposase to “cut” the DNA transposon from the genome and “paste” it into another genomic area. RNA transposons, on the other hand, retain their original positions in the genome and are instead replicated and inserted into another region of the genome via an RNA intermediary (Munoz-Lopez and Garcia-Perez, 2010; Klein and O’Neill, 2019). Notably, at least one study has been able to show that treatment of tau-transgenic Drosophila with reverse transcriptase inhibitors to suppress TEs resulted in marked phenotypic improvement and reduced cell death, presenting a potentially exciting new avenue for therapeutic approaches (Sun et al., 2018).

Recent evidence of isoform-specific biological roles and the appearance of distinct tau isoforms in a variety of diseases led us to hypothesize that tau isoforms may differ in the way they influence DNA integrity, the transcriptome, and the degree and method in which they promote cell death and dysfunction. Moreover, the study by Sun et al. in 2018 suggested that not only might abnormal tau expression promote a novel mechanism of cellular dysfunction via activation of TEs, but that these elements may undergo unique patterns of activation and repression in different types of tauopathies. To this end, we sought to investigate how overexpression of different tau isoforms, which form a basis for separate tau-related diseases, might distinctly affect TE expression.

To address these questions, we utilized cell culture of differentiated neuroblastoma SH-SY5Y cells infected with lentiviruses of different tau isoforms to discover if 3R and 4R tau isoforms produced changes in tau localization, DNA damage, cell death, and the transcriptome, including changes in activation and repression of TEs. Because AD is one of the most prevalent neurodegenerative diseases, we also characterized these phenomena as they occur when beta-amyloid (Aβ) is present. To validate our transcriptomic findings, we repeated our RNA-seq analysis on publicly available human data from AD, PSP, and non-demented patients and found differences in activated and repressed transcriptional pathways among all groups. As our studies confirmed a link between tau and global TE expression, we expanded our TE analysis to quantify TE expression in a locus-specific way in order to further elucidate where TE expression is originating in the genome. Thus our study provides new data suggesting a tau isoform-dependent difference in TE activation and repression, and additionally identifies the locations of activated and repressed TE as expressed in vitro and in human tauopathy samples.

Methods

Construction of lentivirus vectors

The human 3RTau (0N3R, 352) [L266V, G272V] cDNA (Rockenstein, Overk et al. 2015) or 4RTau (1N4R, 412) cDNA Open Biosystems were PCR amplified and cloned into the third-generation self-inactivating lentivirus vector (Tiscornia, Singer et al. 2006) with the CMV promoter driving expression producing the vector. Lentiviruses expressing tau (LV-3Rtau, LV- 4RTau), and empty vector (LV-Ctrl) were prepared by transient transfection in 293T cells (Tiscornia, Singer et al. 2006). For further details on LV-Ctrl production, see previously described methods (Spencer, Michael et al. 2013).

Cell culture

For these experiments, we used the SH-SY5Y human neuroblastoma cell line, which expresses normal levels of human tau and is a widely used in vitro system for modeling neurodegenerative diseases (Xicoy et al., 2017). Undifferentiated cell cultures underwent fewer than 20 passages, were passaged weekly, and were maintained with media composed of 10% fetal bovine serum and a 1:1 mixture of Eagle's Minimum Essential Medium (MEM) and Ham's F12 (F12). In all experiments, cells were infected at plating with at a multiplicity of infection (MOI) of 20, and media was replaced the morning after plating. Cells were infected with LV-Ctrl, LV-3Rtau, LV-4Rtau, or an equal ratio of LV-3Rtau and LV-4Rtau. These were meant to create either a control group or groups overexpressing 3R tau, 4R tau, or both 3R and 4R tau, respectively.

Cells were differentiated for 9 days with media made up of 15 nM Retinoic Acid (Sigma), 3% fetal bovine serum, and 1:1 MEM:F12, which was replaced every 1–2 days. On the 8th day, 24 hours before collection, all cells were treated with either 50 nM oligomeric Aβ-42 (rPeptide, cat no: A-1163), prepared according to previously published methods (Stine et al., 2011) or DMSO.

For a schema of the cell culture infection and treatment procedure, see Fig. 1B.

Subcellular fractionation and Western blot

Cells were plated at onto 10 cm dishes and were treated as previously described. After 24 hours of incubating with Aβ-42, cells were collected and separated into nuclear and cytoplasmic fractions according to Abcam's online subcellular fractionation protocol (https://www.abcam.com/protocols/subcellular-fractionation-protocol). After protein concentrations for all fractions were determined using a reducing agent-compatible BCA assay (ThermoFisher, cat no. 23252), 12.1 ug of protein from each sample was loaded into the wells of a 10% Tris-Glycine gel (Biorad, cat no. 4561034). After gels were run, protein was transferred onto a PVDF membrane and blocked for one hour with 5% BSA in 0.1% Tween/1xTBS. Membranes were then incubated in blocking solution with primary antibodies 4R tau (Millipore Sigma, cat no. 05-804), 3R tau (Millipore Sigma, cat no. 05-803), GAPDH (Abcam, cat no. 181602), and Histone 3 (Abcam, cat no. ab1791) overnight at 4 degrees Celsius, washed, and incubated in blocking solution with respective secondary HRP antibodies (mouse or rabbit) at 1:5000 for one hour at room temperature before a final wash step and imaging using West Pico Supersignal (ThermoFisher, cat no. 34580)

Immunofluorescence and confocal microscopy

Cells were plated onto glass poly L-lysine-coated coverslips into 12-well cell culture plates and infected and differentiated as described previously. Following Aβ-42/DMSO treatment, coverslips were washed once with ice-cold 1xPBS and fixed with ice-cold 4% PFA.

All combinations of LV-tau and Aβ-42/DMSO treatment were assessed via immunofluorescent staining and confocal microscopy. Coverslips were washed with 1xPBS, followed by 1 hour of blocking with 3% normal goat serum in 0.2% Triton-X/1xPBS. Samples were then incubated with a primary antibody in blocking solution overnight at 4 degrees Celsius. Following incubation, samples were again washed with 1xPBS, incubated with anti-rabbit Alexa Fluor 568 secondary antibody for 2 hours, then washed again with 1xPBS and 0.2% Triton-X/1xPBS before being counterstained with DAPI and mounted. The following primary antibodies were used: 1:500 anti-rabbit yH2AX (Bethyl Laboratories, cat no. A300-081A-M) and 1:500 polyclonal rabbit, anti-human tau (Dako, cat no. A0024).

All slides were imaged with a DMI 4000B inverted fluorescent microscope (Leica, Germany) with an attached TCS SPE confocal system (Leica), using a Leica 63X (N.A. 1.3) objective. Analysis of images was carried out using Fiji. For samples stained for yH2AX, nuclei were selected using the DAPI/blue channel and traced by hand, excluding nuclei cut off by the edges of the image or that overlapped with each other or with neurites; nuclear foci were quantified using an online protocol provided by Duke University Microscopy Core with a maxima threshold determined using secondary-only

control images in order to distinguish true signal from background. For samples stained for tau, cells were segmented by hand into nuclear (with DAPI staining as a reference) and cytoplasmic (defined as the area of the cell outside the nucleus) regions and corrected total cell fluorescence (CTCF) was calculated each region. The ratio of CTCF coming from the nucleus versus the cytoplasm was then assessed to determine total tau localization within the cell. Statistical significance for both datasets was assessed using a Wilcoxon ranked-sum test and multiple testing corrections were done using the False Discovery Rate. Figures were created with the R package ggplot2.

Cytotoxicity

The CellTox™ Green Cytotoxicity Assay (Promega, cat no. G8742) was used according to the manufacturer's instructions to assess cytotoxicity as the result of LV-tau infection and Aβ-42 treatment. Cells were plated and infected into three 96-well cell culture plates. Because the assay allows for fluorescence to be measured for up to 72 hours, each plate was used to measure cell death over a period of 2–3 days, for a total of 9 days (the time period of differentiation for all cells). The first plate was designed to measure cell death resulting from infection over the first 3 days after plating (the assay was started after media was replaced following plating) (N=14), the second plate for days 4–6 after plating and infection (N=14), and the third plate was used to measure cell death as a result of infection and Aβ-42 treatment over days 8–9 (N=7). Cells were fed every 72 hours or when the assay for each plate was performed.

Figures were generated using the R package ggplot2, and statistical significance was assessed using a Wilcoxon ranked-sum test, with multiple testing corrections done using the False Discovery Rate.

RNA isolation and library preparation

Cells were plated and infected in triplicate into 6-well cell culture plates. Following treatment with Aβ-42 and DMSO, cells were scraped from the plates and their RNA was collected using TRIzol (Invitrogen, cat no. 10296010) according to the manufacturer's instructions.

RNA quality checking, library preparation and sequencing were conducted at the IGM Genomics Center, University of California, San Diego, La Jolla, CA. All RNA had at least an RNA integrity score of 7.9, with the majority of samples scoring greater than 9.5. Libraries were constructed using poly(A) selection to generate 100 bp paired-end reads and were sequenced with an Illumina NovaSeq 6000 that was purchased with funding from a National Institutes of Health SIG grant (#S10 OD026929).

Publicly available RNA-sequencing data from AD, PSP, and control patients (obtainable through AMP-AD Knowledge Portal, doi:10.1038/sdata.2016.89) were also analyzed. For details on how this data was generated, see Allen et al., 2016.

RNA-seq processing and analysis

Sequencing quality for all FASTQ files was obtained via FastQC (Andrews, 2010) both before and after adapter removal using BBduk (BBMap_38.73, https://jgi.doe.gov/data-and-tools/bbtools/bb-tools-user-guide/bbduk-guide/). FASTQ

files were then mapped to the GRCh38 human reference genome and GTF (release number 98) available through Ensembl using STAR (version 2.7.3a, Dobin et al., 2013). Qualimaps (v2.2.1, Okonechnikov et al., 2016) was used to visualize the quality of resulting bam files. Gene counts were determined through featureCounts from the package Subread (version 1.6.4, Liao et al., 2014), differential gene expression was computed using DESeq2 (version 1.26.0, Love et al., 2014), and GO analysis was carried out using clusterProfileR (Yu et al., 2012).

TEcount and TElocal, from the Hammell lab's TEtoolkit suite, were used to determine transposable element expression. TEcount (Jin et al., 2015) was used in order to produce a global view of TE expression and TElocal to show localized TE expression, following the alignment protocol and settings described by the authors (Jin and Hammell, 2018), with the maximum number of iterations set to 100 (the default).

Publicly available FASTQ data generated from the temporal cortex of AD, PSP, PA, and non-demented control patients obtainable through the AMP-AD Knowledge Portal (doi:10.1038/sdata.2016.89) were downloaded from Synapse using the R package synapser (https://github.com/Sage-Bionetworks/synapser). These FASTQ files were selected based on RNA integrity number (>8.0) and quality assessment with FastQC to yield a total analyzed sample size of 60 AD, 71 PSP, and 33 control patients. All selected FASTQ files then underwent the same RNA-seq processing and analysis as FASTQ files generated from cell culture. Covariate data was also downloaded from the AMP-AD Knowledge Portal, and biological and technical covariates — gender, brain bank (referred to as "Source), and the flowcell used for sequencing — were accounted for when fitting the model used by DESeq2.

Results

Lentivirus infection of SH-SY5Y neuroblastoma cells yields isoform-specific overexpression of tau

Cell culture of the human SH-SY5Y neuroblastoma cell line is a widely used in vitro system for modeling neurodegenerative diseases (Xicoy et al., 2017). To generate overexpression of non-mutant tau isoforms, we infected SH-SY5Y cells at an MOI of 20 with lentiviruses encoding 0N3R and 1N4R tau isoforms and differentiated cells with 15nM RA for 9 days. On the 8th day of differentiation, cells were treated either with 50 nM Aβ-42 oligomers to form a model of Alzheimer's disease (characterized by overexpression of tau isoforms and presence of toxic Aβ species) or with an equal concentration of DMSO to serve as a control. For an overview of cell culture procedures, see Fig. 1B.

After collection, cells underwent subcellular fractionation to observe tau expression in both the nucleus and cytoplasm, and Western blots were carried out using 3R and 4R tau isoform-specific antibodies to validate the experimental model (N=1). As expected, cell cultures treated with LV-3Rtau displayed overexpression of 3R tau relative to other groups, while those treated with LV-4Rtau showed distinct overexpression of 4R tau. Control groups displayed neither overexpression of 3R tau nor 4R tau. Histone 3 (H3) and GAPDH were used as loading controls for nuclear and cytoplasmic fractions, respectively (Fig. 1A).

Tau isoform overexpression and treatment with Aβ do not result in different nuclear/cytoplasmic total tau ratios.

Loss of tau in the nucleus is associated with increased DNA damage and disruptions in heterochromatin organization (Violet et al., 2014; Mansuroglu et al., 2016). Moreover, there is evidence that Aβ may influence the localization of tau within neurons (Zempel et al., 2010). To ascertain whether a gain or loss of overall tau protein within the nucleus of differentiated SH-SY5Y cells occurred in the context of 3R or 4R tau overexpression and Aβ treatment, we performed immunofluorescence staining for total tau to assess potential different tau isoform-induced nuclear changes. Images were taken with a confocal microscope (Fig. 2A) and analysis was carried out using Fiji and R. To assess the movement of tau into or out of the nucleus, we quantified the ratio of CTCF tau signal in the nucleus and in the cytoplasm. Overall, we found no significant differences in the ratio of tau expression in the nucleus or cytoplasm in tau-treated samples versus control samples (Fig. 2B) (N=3).

Tau isoform overexpression results in significantly fewer DNA double-strand breaks.

Despite a lack of tau redistribution within differentiated SH-SY5Y cells, we found significant decreases in DNA double-strand breaks (DSBs) in tau-treated samples versus control samples (N=3) (Fig. 3B). Notably, this phenomenon was most prevalent in samples treated with LV-4Rtau alone ($p=0.037$) or with Aβ ($p=0.014$) and completely absent in samples treated only with LV-3Rtau or equal amounts of LV-3Rtau and LV-

4Rtau. Treatment with Aβ also appeared to have a slightly protective effect when given either to control samples (p=0.049) or to LV-3Rtau samples (p=0.014).

Overexpression of 3R tau results in a consistent pattern of cell death.

Next, we examined whether overexpression of tau isoforms resulted in differences in cell death. Using the CellTox Green Cytotoxicity Assay from Promega, which utilizes a green fluorescent dye to assess membrane damage (and thus cell nonviability), we quantified cell death across each experimental condition on each day of a typical differentiation procedure, excluding the first day when cells were infected and plated in 96-well plates. Because the fluorescent dye lasts for 72 hours, cells were segmented into three separate plates signifying three groups: Plate 1 measured cell death from the time lentiviruses were taken off the cells (Day 2) through Day 4 of the differentiation procedure, Plate 2 measured cell death from Days 5–7, and Plate 3 measured cell death as a result of Aβ treatment on each lentivirus condition (Days 8–9) (see Fig. 4A for a schema of the workflow). Statistical analysis revealed a relatively consistent pattern of significant cell death associated with LV-3Rtau infection on most (6 out of 8) days measured (N=14); LV-3Rtau infection also showed higher levels of cell death compared to LV-4Rtau infection and 1:1 LV-3Rtau:LV-4Rtau infection groups, especially during Days 5–7 (Fig. 4B). Notably, LV-4Rtau infections resulted in increases in cell death on Days 5, 6, and 9, while 1:1 LV-3Rtau:LV-4Rtau infections only showed increased cell death on Day 5. Aβ treatment did not appear to significantly affect cell viability in any group (Fig. 4C–D). Although Aβ treatment appears to result in a significant increase in cell death in LV-3Rtau infections, this must be interpreted with

caution because the DMSO-treated LV-3Rtau infection group shows significantly lower cell death from Days 8–9, implying that either Aβ does in fact have a deleterious interaction with 3R tau or that this result is an artefact of variation in the DMSO-treated group.

Tau isoforms, AD, and PSP produce uniquely altered gene expression.

To examine potential mechanisms behind tau-mediated cellular dysfunction, we carried out 100 bp paired-end RNA-sequencing of cell culture samples (N=3). In addition, we analyzed 100 bp paired-end RNA-sequencing data from human patients with AD (N=60), PSP (N=71), and without any neurodegeneration (N=33) (Allen et al., 2016). Principal component analysis revealed distinct groupings between samples infected with tau lentiviruses and control samples, with less clear delineation between Aβ and DMSO-treated cultures (Fig. 5A). AD patients' data were similarly separated from control patients' data, though PSP cases appeared less divided from controls (Fig. 5B).

AD cases showed the greatest number of significantly differentially expressed genes, with PSP cases showing far fewer (Fig. 5D). Among the cell culture samples, those infected with 1:1 LV-3Rtau:LV-4Rtau displayed the greatest number of DEGs, followed by LV-4Rtau samples, and then LV-3Rtau samples. The samples infected with LV-Ctrl and treated with Aβ (the Aβ-only samples) showed the fewest significantly differentially expressed genes by far, with only 5 reaching the significance level of an adjusted p-value < 0.05. Overall, AD cases appeared to follow a distinct pattern of gene expression compared to the rest of the samples, while the cell culture samples

significantly expressed a number of genes that did not meet the significance threshold in either PSP or AD (Fig. 4C).

Gene expression patterns related to synaptic and mitochondrial functions were downregulated in AD, which concurs with the broad range of studies that show dysfunction in these areas in AD patients (Forner et al., 2017; Moreira et al., 2010). Upregulation of pathways pertaining to extracellular structure and focal adhesions were prevalent in all groups except PSP patients. Pathways related to protein synthesis appeared downregulated under all conditions except for AD patients and DMSO-treated LV-3Rtau samples. Downregulation of genetic and epigenetic phenomena occurred in both LV-3R4Rtau samples and in LV-4Rtau samples, while these processes were upregulated in both AD and PSP. Finally, all cell culture groups displayed upregulation — with some also displaying downregulation — of processes related to cell development, negative regulation of neurogenesis, and negative regulation of neuron differentiation (Fig. 5E).

Tau isoforms, AD, and PSP produce distinct activation and repression of transposable elements.

Recent studies suggest that tau may influence activation of TEs, which are mobile DNA sequences that have long been associated with genomic instability and more recently with potential regulatory functions (Guo et al., 2018; Sun et al., 2018; Klein and O'Neill, 2019). To examine how tau isoforms might affect TE activation, we analyzed our RNA-seq data using software tools for identifying differentially expressed TE loci. PCA results show some separation between AD, PSP, and control patients

(Fig. 6B) and distinct groupings among cell culture conditions with small distances between DMSO and Aβ-treated samples (no TE loci were differentially expressed between any DMSO and Aβ-treated samples infected with the same lentivirus) (Fig. 6A). Our analysis further revealed that overexpression of either tau isoform was sufficient to cause at least some TE dysregulation, though TEs appeared more abundantly dysregulated when 4R tau was overexpressed or when 3R tau was overexpressed in the context of Aβ treatment (Fig. 6D). The two families of TEs that represent the most dysregulated loci were the L1 and Alu families, which are classified as part of the LINE and SINE classes, respectively (Fig. 7A–B). The L1 family in particular is considered the only autonomous TE family still active in the human genome, while Alu can be activated by L1 activity (Terry and Devine, 2020). Far greater numbers of TEs showed differential expression in AD and PSP cases compared to cell culture samples, likely reflecting the greater cellular heterogeneity and complexity of bulk RNA-seq data from human brains than from cell culture (Fig. 6D, 7A–B). AD and PSP displayed similar patterns of TE expression, though more TE loci were differentially expressed in AD than in PSP (Fig. 6C, 7A–B). No TEs were differentially expressed in Aβ-treated LV-Ctrl cell cultures, suggesting that TE activation is not solely driven by Aβ, but may be promoted by tau pathology, confirming the results of other studies (Guo et al., 2018).

Discussion

Despite being one of the leading causes of death worldwide, neurodegenerative diseases are notoriously lacking in any kind of therapeutic treatment. Though several toxic forms of proteins are major actors in these types of diseases, abnormal expression of one or more tau protein isoforms is characteristic of a significant portion of them. Mechanisms underlying tau-mediated neurodegeneration and the unique roles of its isoforms remain poorly understood, and recent studies have shown that tau may play more diffuse roles in the cell than binding to microtubules. Creating a fuller picture of how tau and its isoforms may lead to neurodegeneration is thus critical for designing treatments for tau-based diseases.

In this study, we sought to elucidate differences in how two major types of isoforms, 3R and 4R tau, promote pathways to cellular dysfunction. By analyzing the transcriptomes in a cell culture model of tau isoform overexpression, we demonstrated that 3R and 4R tau isoforms, when overexpressed alone or in combination with each other and with Aβ, promoted markedly different transcriptomic patterns. Notably, while no combination of tau isoform overexpression and Aβ is sufficient to recapitulate all dysregulated pathways seen in our analysis of RNA-seq data from AD and PSP patients, overexpression of either isoform is sufficient to cause dysregulation in TE expression, though this effect is more prominent with 4R tau overexpression. Only when Aβ was introduced did the 3R tau samples start to replicate the patterns of TE expression seen in AD, PSP, and the other cell samples. Interestingly, the LV-Ctrl group treated with Aβ alone failed to show any dysregulated TE expression, implying that while Aβ alone may not be sufficient to drive TE dysregulation, it appears to aggravate

aberrant TE expression in the context of tauopathy. This pattern of dysregulated TE expression in cells also paralleled our findings in the RNA seq analyses in the clinical samples in which both AD and PSP patients samples had dysregulated TE expression but the AD patient samples appeared to have higher dysregulated TE expression than the PSP patient samples. This is consistent with greater dysregulation of TE expression with 3R4R tau in the presence of Aβ as featured in AD but to a lesser degree with PSP (4R tau in the absence of Aβ). Recent evidence shows that tau pathology can broadly impact the epigenome through heterochromatin relaxation and histone acetylation (Frost et al., 2014; Guo et al., 2018; Klein et al., 2019). Mechanistically, then, it stands to reason that tau-driven epigenetic changes could lead to TE dysregulation (Guo et al., 2018, Sun et al., 2018). To our knowledge, our study is the only one to examine the transcriptomes of overexpressed 3R and 4R tau isoforms in interaction with Aβ, and to show a tau isoform-dependent change in TE dysregulation. TE dysregulation has only recently been discovered in tauopathies, and has been garnering attention in other neurodegenerative diseases (Tam et al., 2019).

Despite the current lack of research on TEs in neurodegeneration, one study has shown that in a tauopathy model of Drosophila, treatment with a reverse transcriptase inhibitor reduces TE activation and increases longevity (Sun et al., 2018). In our study, the two TE families with the greatest number of dysregulated loci were the L1 and Alu families. Intriguingly, these two families are main suspects in the pathogenesis of other neurological diseases. Both, for instance, are implicated in Aicardi-Goutieres Syndrome, which is characterized by neuroinflammation driven by increased type I-interferon activity (Tam et al., 2019). Links between L1 expression and the dedifferentiation of

cells in AD have also been drawn (Tam et al., 2019). If TE dysregulation does in fact promote neurological damage in a variety of diseases, this could provide a novel and actionable avenue for therapeutic interventions.

Aside from dysregulation in TE expression, several notable phenomena emerged from our RNA-seq analysis. Gene Ontology (GO) overrepresentation analysis revealed downregulation of several processes related to protein synthesis and the ribosome in PSP and most other cell samples. Tau-mediated disruption in protein synthesis has been previously noted to be a contributing factor to neurodegeneration (Meier et al., 2016). Terms related to structural components of the cell, such as the extracellular matrix and adherence junctions, were also largely upregulated in AD and the cell groups, as might be expected given the role of tau in cytoskeletal organization. As in TE expression, the presence of Aβ appears to drive the LV-3Rtau group toward transcriptomic patterns that converge with those of LV-4Rtau and LV-3R4Rtau groups.

Other aspects of our study also showed interesting divergence in tau isoform-driven effects. For instance, 3R tau consistently showed higher cytotoxicity levels compared to control groups than did other samples, and occasionally showed higher toxicity than either the LV-3R4R or LV-4R groups. These results concur with literature suggesting that the 0N3R tau isoform led to shorter lifespans in transgenic Drosophila (Sealey et al., 2017), but contrast with other studies which conclude that 4R tau overexpression is more pathogenic, especially in htau transgenic mice (Schoch et al., 2016). While greater clarification is needed on this issue, the existence of both 3R and 4R tauopathies suggest that overexpression of either isoform is ultimately toxic. Ultimately, researching mechanisms of how these isoforms produce cytotoxicity may prove more fruitful, and

recent research has illuminated how overexpression of either isoform can lead to opposite disruptions in vesicle transport (Lacovich et al., 2017). More surprisingly, the 1:1 combination of 3R and 4R tau in our model showed relatively low levels of cytotoxicity compared to controls. Relatively high spread in the distributions of all groups may partially account for this, and either a more sensitive assay or higher numbers of samples may be called for when assessing cytotoxicity in response to these isoforms over several days. Alternatively, it may be that the equal overexpression of both isoforms requires more time to show its cytotoxic effects; the LV-3R4R tau groups showed much greater transcriptional dysregulation than the other groups, which suggests that these groups are in fact being affected by their overexpression of both isoforms. Notably, these samples also showed the strongest dysregulation of TEs among all cell culture groups and followed a similar pattern of TE disruption found in AD and PSP. Whether these transcriptional changes eventually manifest in greater cytotoxicity remain to be seen.

We also sought to determine whether isoform-specific tau overexpression had any effect on the prevalence of DSBs, which are highly damaging to cells and have been found to be increased in the brains of people with AD and mild cognitive impairment (Shanhbag et al., 2019). Tau deficiency has been previously linked to DNA damage, and overexpression of tau in tau-deficient models has been shown to decrease DNA damage (Sultan et al., 2011; Violet et al., 2014). Though our data was characterized by high levels of variation and outliers, we found that overexpression of the 4R tau isoform in particular resulted in fewer DSBs as measured by yH2AX fluorescence. Notably, changes in DSBs in our cell models could not be correlated with

any change in the ratio of nuclear vs. cytoplasmic levels of tau, as no samples showed any significant translocation of tau, although we did not assess whether there was any change in localization of tau isoforms. This result did not exclude the possibility of tau isoforms affecting DNA integrity or chromatin organization, as more subtle pathways affecting these components may be involved, but led us to conclude that relative tau distribution from the nucleus to the cytoplasm is unaffected by Aβ treatment or overexpression of certain tau isoforms.

Overall, our study illuminates several distinctions in how 3R and 4R tau isoforms may disrupt normal cellular function and reveals that TE dysregulation can result from overexpression of non-mutant human tau isoforms, with expression patterns recapitulating those of AD and PSP. Our study shows both locus-specific TE and global TE expression patterns in context of tau isoform overexpression and in AD and PSP cases. The only other two studies to examine TE expression in AD have concluded that LTR families of TEs are the most dysregulated; however, these studies depended on taking a global view of TE expression, instead of a locus-specific one (it should be noted that software for locus-specific TE detection was likely not available for these studies, as it has only recently been developed). Our own global view of TE expression largely confirms the pattern of their results, yet interestingly, when viewed from a locus-specific standpoint, L1 and Alu families are far better represented among the dysregulated TEs. This is particularly notable given that L1 in particular is the only active and autonomous TE family in humans, while Alu is an active element that hijacks L1 replicative machinery. These results will eventually need more stringent validation than is currently available; repetitive DNA regions, which describe most TEs, are notoriously difficult to

call in current short-read sequencing platforms, and long-read platforms, while promising, have issues with error rates and read depth to overcome (O'Neill et al., 2020). Since both the number of dysregulated TE loci and the number of dysregulated TE families remains much higher in AD and PSP than in our cell culture models, it is likely that there are other mechanisms also at play in TE expression in disease. Because our cell model only evaluated neuronal cells, it would be illuminating to see how TE expression might differ among the other cell types known to be affected by aberrant tau. Moreover, the link between tau pathology and epigenetic changes provides a possible mechanism for tau-induced TE differential expression, meriting a more data-intensive look at how tau and its isoforms affect chromatin remodeling than has previously been performed. Overall, the evidence supporting the notion that TE dysregulation could be a cytotoxic, therapeutically targetable consequence of pathogenic tau offers a new, exciting vantage point into the nature of tauopathic diseases.

Figures

A.

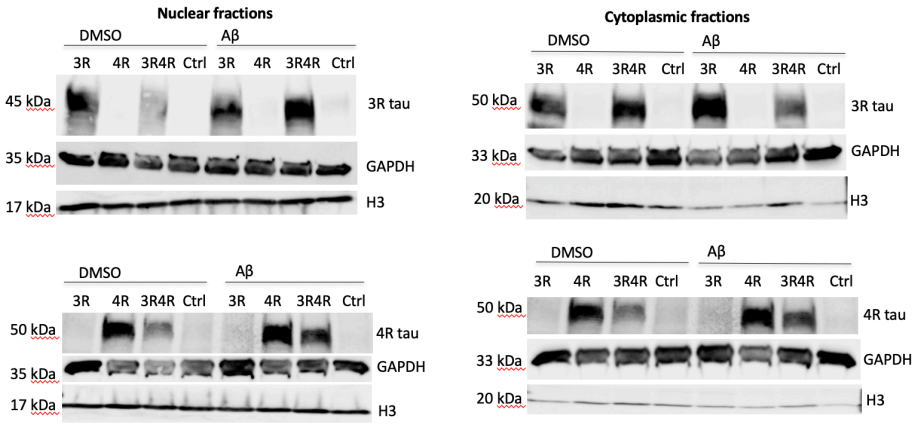

B.

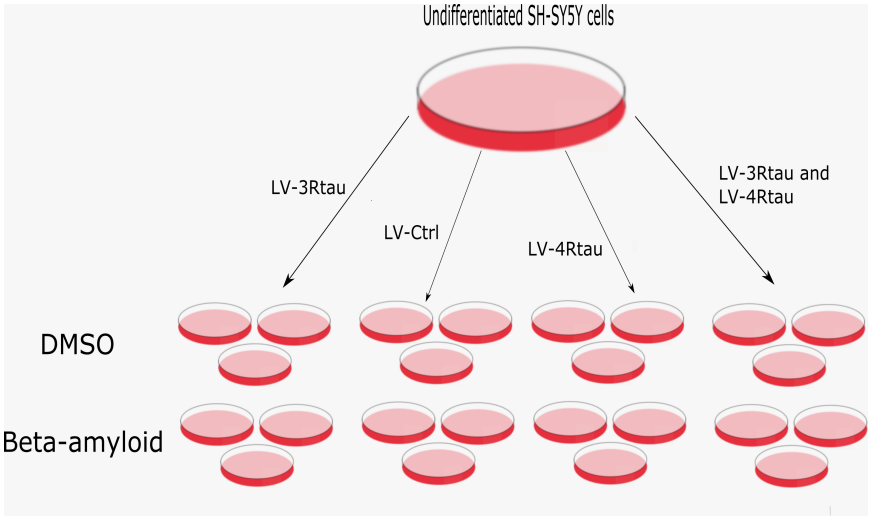

Figure 1. Validation of a typical infection and treatment workflow. A. Use of tau isoform-specific antibodies in Western blotting shows tau isoform-specific overexpression in both nuclear and cytoplasmic fractions as a result of infection with tau lentiviruses. **B.** A typical workflow for infecting cells with N=3. Cells were treated with 50nM Aβ or DMSO 24 hours before collection.

A.

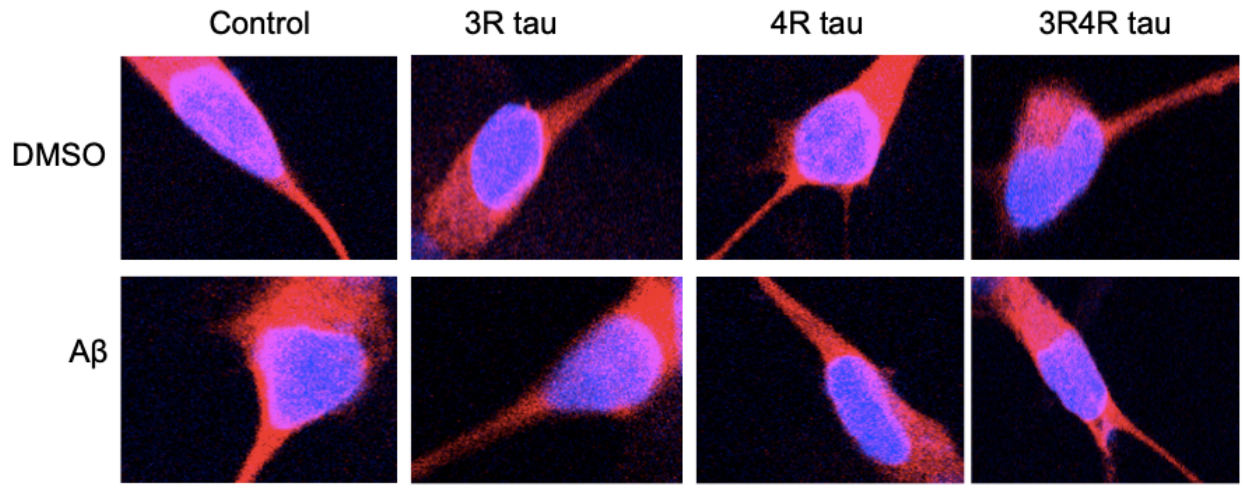

B.

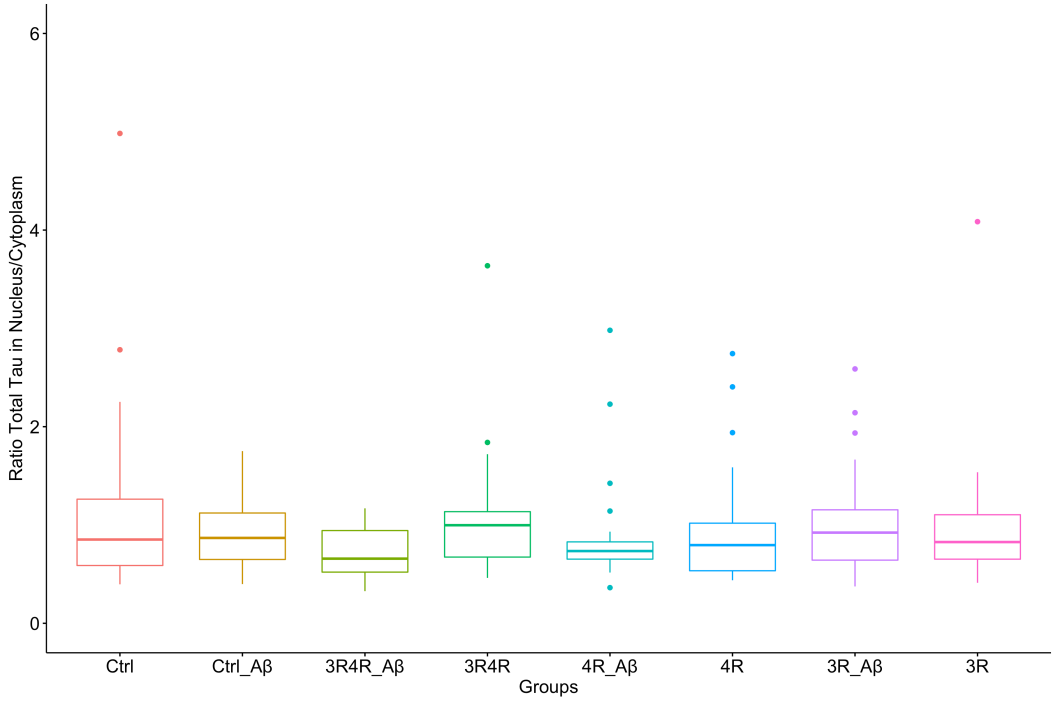

Figure 2. Total tau ratio between nucleus and cytoplasm is unchanged by overexpression of tau isoforms and Aβ. A. Confocal images of representative total tau (red) stained samples with nuclei stained with DAPI (blue). **B.** No significant changes are seen across groups in the nuclear/cytoplasmic ratio of total tau signal (N=3).

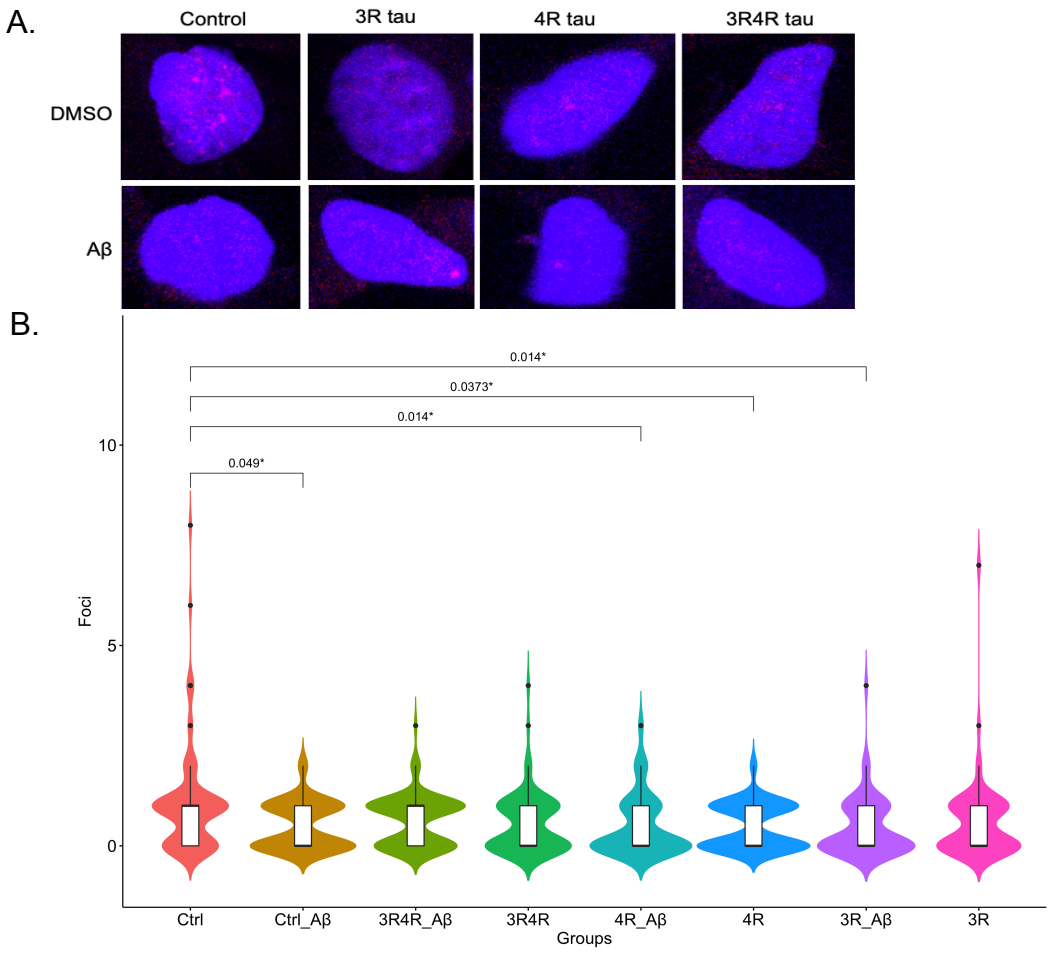

Figure 3. Overexpression of certain tau isoforms appears to lower DSB occurrence. A. Confocal images (63x objective) of representative yH2AX (red) stained samples with nuclei stained with DAPI (blue). Red nuclear foci indicate places where DSBs have formed. **B.** 4R tau overexpression, 3R tau overexpression with Aβ treatment, and Aβ treatment of LV-Ctrl groups appear to correlate with smaller DSB distributions relative to control (N=3).

Figure 4. Cytotoxicity of tau isoforms and their interactions with Aβ. A. Diagram explaining cytotoxicity assay workflow; plates 1 and 2 measured cytotoxicity through days 2–7, while plate 3 measured cytotoxicity on days 8–9, which captured cytotoxicity changes due to Aβ treatment. **B.** Comparison of fluorescence values (cytotoxicity proxy, with higher fluorescence signifying greater levels of cell death) over days 2–7 for LV-Ctrl, LV-3R4Rtau, LV-4Rtau, and LV-3Rtau groups. Multiple comparison correction was done using FDR. **C.** Comparison of fluorescence/cytotoxicity between LV-Ctrl treated with DMSO, LV-Ctrl treated with Aβ, LV-3Rtau treated with Aβ, and LV-3Rtau treated with DMSO on days 8–9, plate 3. Multiple comparison correction was done using FDR. **D.** Comparison of fluorescence/cytotoxicity between LV-Ctrl treated with DMSO, LV-Ctrl treated with Aβ, LV-4Rtau treated with Aβ, and LV-4Rtau treated with DMSO on days 8–9, plate 3. Multiple comparison correction was done using FDR. **Note:** No significant changes were seen in the comparison between LV-Ctrl treated with DMSO, LV-Ctrl treated with Aβ, LV-3R4Rtau treated with Aβ, and LV-3R4Rtau treated with DMSO on days 8–9, plate 3. Data not shown.

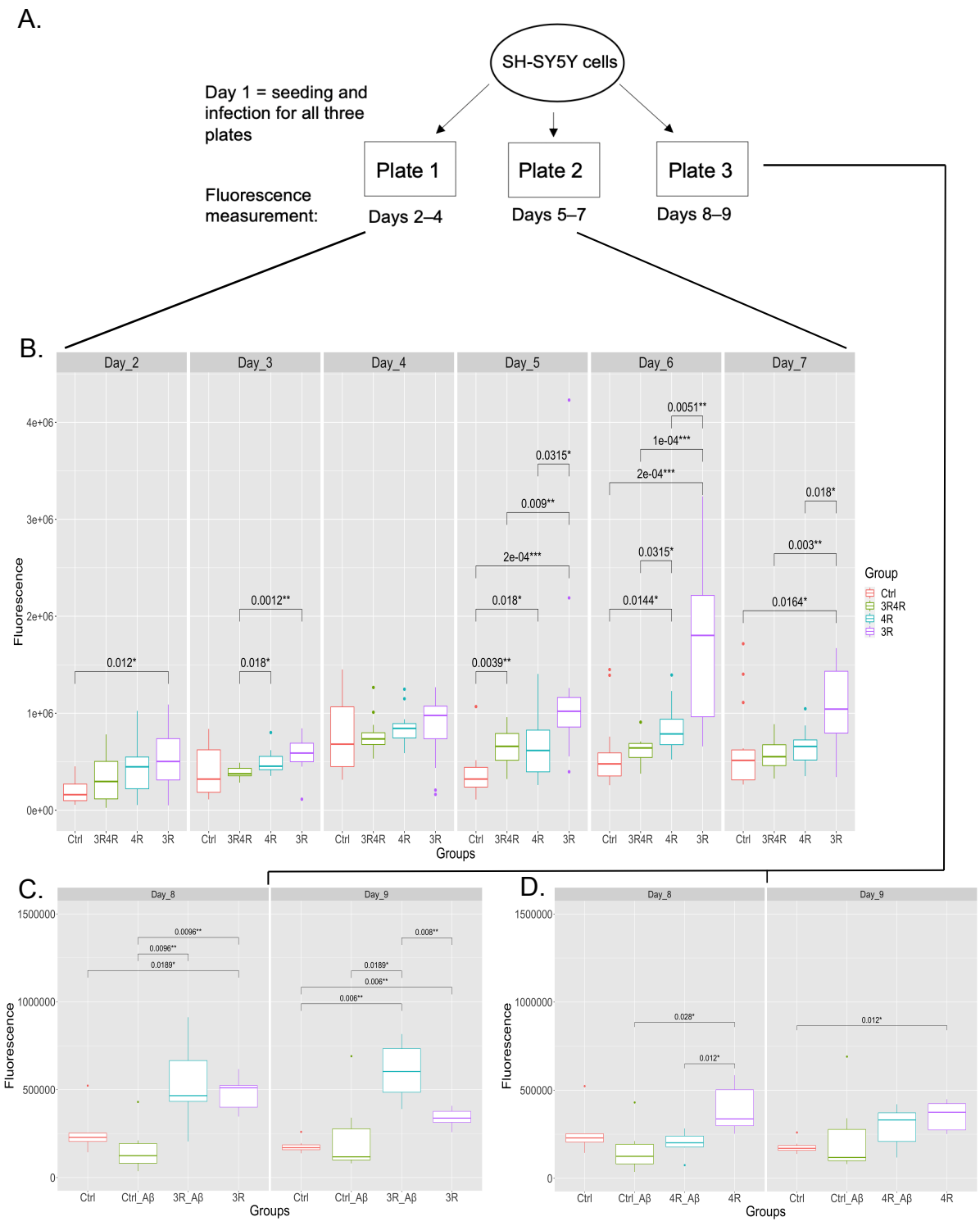
A.
SH-SY5Y cells
Day 1 = seeding and infection for all three plates
Plate 1
Plate 2
Plate 3
Fluorescence measurement:
Days 2–4
Days 5–7
Days 8–9
B.
Day_2
Day_3
Day_4
Day_5
Day_6
Day_7
Fluorescence
Groups
Ctrl
3R4R
4R
3R
Group
C.
Day_8
Day_9
Ctrl
Ctrl_Aβ
3R_Aβ
3R
D.
4R_Aβ
4R

Figure 5. Patterns in differentially expressed genes in AD, PSP, and cell models. **A.** PCA displaying grouping by gene expression between lentivirus and treatment conditions; PC1 accounts for 81% of variation between conditions, and there is little separation between Aβ and DMSO-treated groups (N=3). **B.** PCA displaying grouping by gene expression between AD (N=60), control (N=33), and PSP (N=71) patients. PC1 accounts for 28% of variation, with AD patients showing greater separation from control patients than PSP patients do. **C.** Heatmap showing log-fold change in expression in genes considered significantly differentially expressed (adjusted p-value<0.05) in each measured group (AD, N=60; PSP, N=71; cell groups, N=3 each) relative to their respective controls (control patients, N=33 for human disease cases; LV-Ctrl cells for cell conditions, N=3). White spaces indicate missing gene data, i.e., the genes were not significantly differentially expressed in these groups. LV-Ctrl treated with Aβ cell model is not shown due to too few significantly differentially expressed genes; these genes can be found in Supplementary Materials. **D.** Table showing the number of significantly differentially expressed genes (adjusted p-value<0.05) in each condition measured. **E.** Overrepresentation analysis of gene-ontology enriched biological processes, molecular functions, and cellular components, with top 30 terms shown.

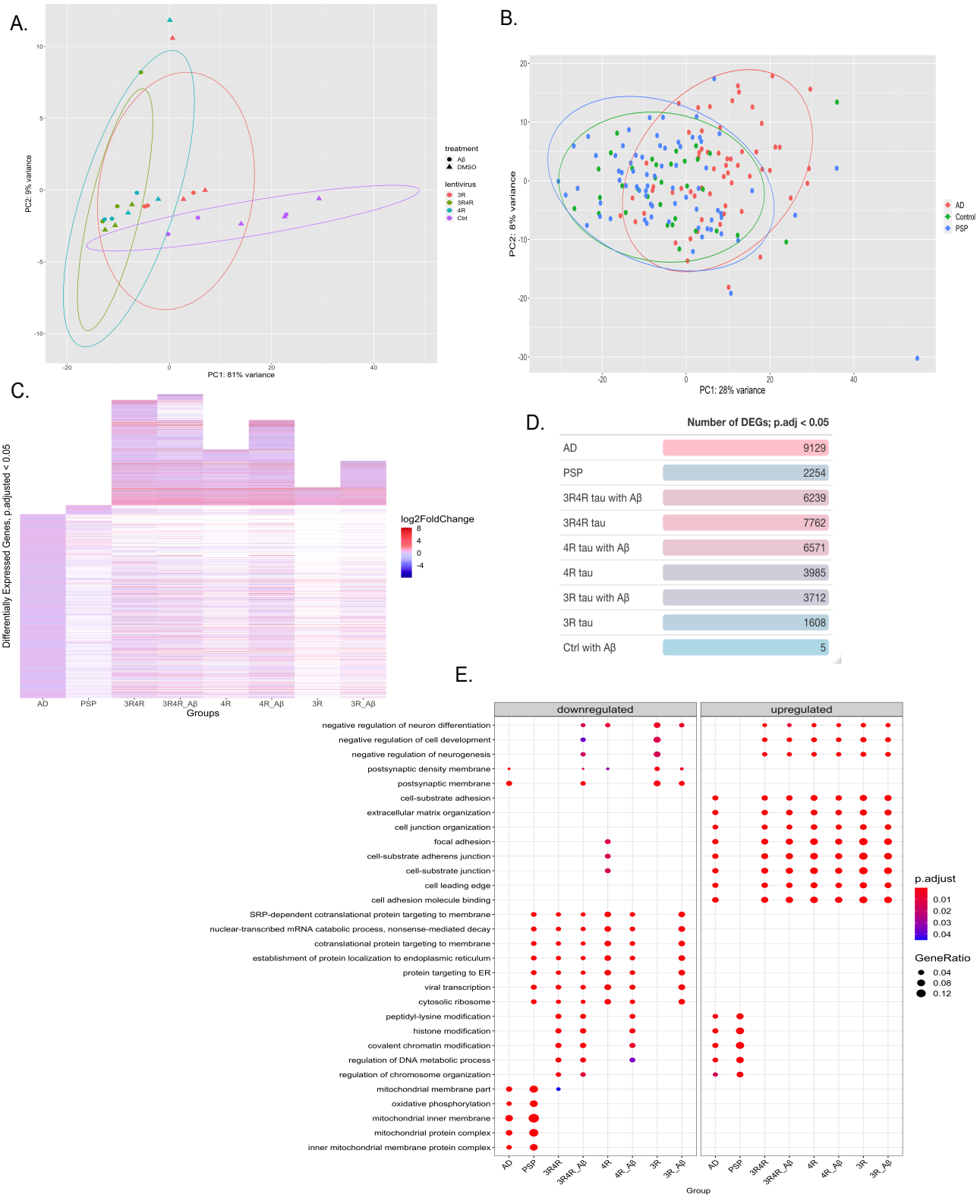
A.
PC2: 9% variance
PC1: 81% variance
treatment
Aβ
DMSO
lentivirus
3R
3R4R
4R
Ctrl
B.
PC2: 8% variance
PC1: 28% variance
AD
Control
PSP
C.
Differentially Expressed Genes, p.adjusted < 0.05
log2FoldChange
Groups
AD
PSP
3R4R
3R4R_Aβ
4R
4R_Aβ
3R
3R_Aβ
D.
Number of DEGs; p.adj < 0.05
AD 9129
PSP 2254
3R4R tau with Aβ 6239
3R4R tau 7762
4R tau with Aβ 6571
4R tau 3985
3R tau with Aβ 3712
3R tau 1608
Ctrl with Aβ 5
E.
downregulated
upregulated
negative regulation of neuron differentiation
negative regulation of cell development
negative regulation of neurogenesis
postsynaptic density membrane
postsynaptic membrane
cell-substrate adhesion
extracellular matrix organization
cell junction organization
focal adhesion
cell-substrate adherens junction
cell-substrate junction
cell leading edge
cell adhesion molecule binding
SRP-dependent cotranslational protein targeting to membrane
nuclear-transcribed mRNA catabolic process, nonsense-mediated decay
cotranslational protein targeting to membrane
establishment of protein localization to endoplasmic reticulum
protein targeting to ER
viral transcription
cytosolic ribosome
peptidyl-lysine modification
histone modification
covalent chromatin modification
regulation of DNA metabolic process
regulation of chromosome organization
mitochondrial membrane part
oxidative phosphorylation
mitochondrial inner membrane
mitochondrial protein complex
inner mitochondrial membrane protein complex
Group
p.adjust
GeneRatio

Figure 6. Patterns of locus-specific transposable element expression across human disease and cell samples. A. PCA displaying grouping by locus-specific TE expression between lentivirus and treatment conditions; PC1 accounts for 36% of variation between conditions (N=3). **B.** PCA displaying grouping by locus-specific TE expression between AD (N=60), control (N=33), and PSP (N=71) patients. PC1 accounts for 20% of variation, while PC2 accounts for 17% of variation. **C.** Heatmap showing log-fold change in expression of TE loci considered significantly differentially expressed (adjusted p-value<0.05) in each measured group (AD, N=60; PSP, N=71; cell groups, N=3 each) relative to their respective controls (control patients, N=33 for human disease cases; LV-Ctrl cells for cell conditions, N=3). White spaces indicate missing data, i.e., the TE loci were not significantly differentially expressed in these groups. LV-Ctrl treated with Aβ cell model did not display any differentially expressed TE loci relative to LV-Ctrl and is thus not included in the heatmap. **D.** Table showing the number of significantly differentially expressed TE loci (adjusted p-value<0.05) in each condition measured.

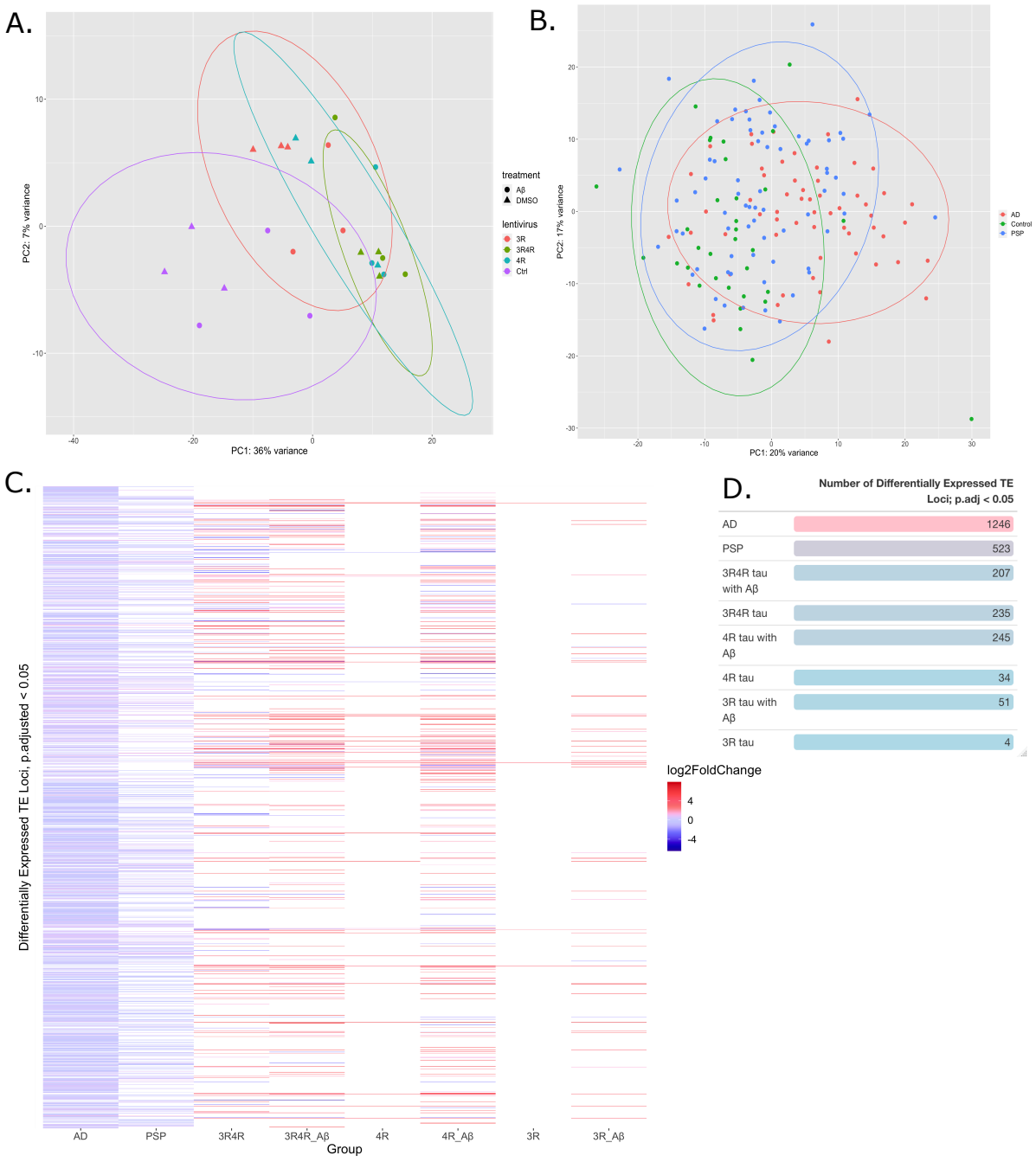
A.
PC2: 7% variance
PC1: 36% variance
treatment
Aβ
DMSO
lentivirus
3R
3R4R
4R
Ctrl
B.
PC2: 17% variance
PC1: 20% variance
AD
Control
PSP
C.
Differentially Expressed TE Loci, p.adjusted < 0.05
AD
PSP
3R4R
3R4R_Aβ
4R
4R_Aβ
3R
3R_Aβ
Group
log2FoldChange
4
0
-4
D.
Number of Differentially Expressed TE Loci; p.adj < 0.05
AD 1246
PSP 523
3R4R tau with Aβ 207
3R4R tau 235
4R tau with Aβ 245
4R tau 34
3R tau with Aβ 51
3R tau 4

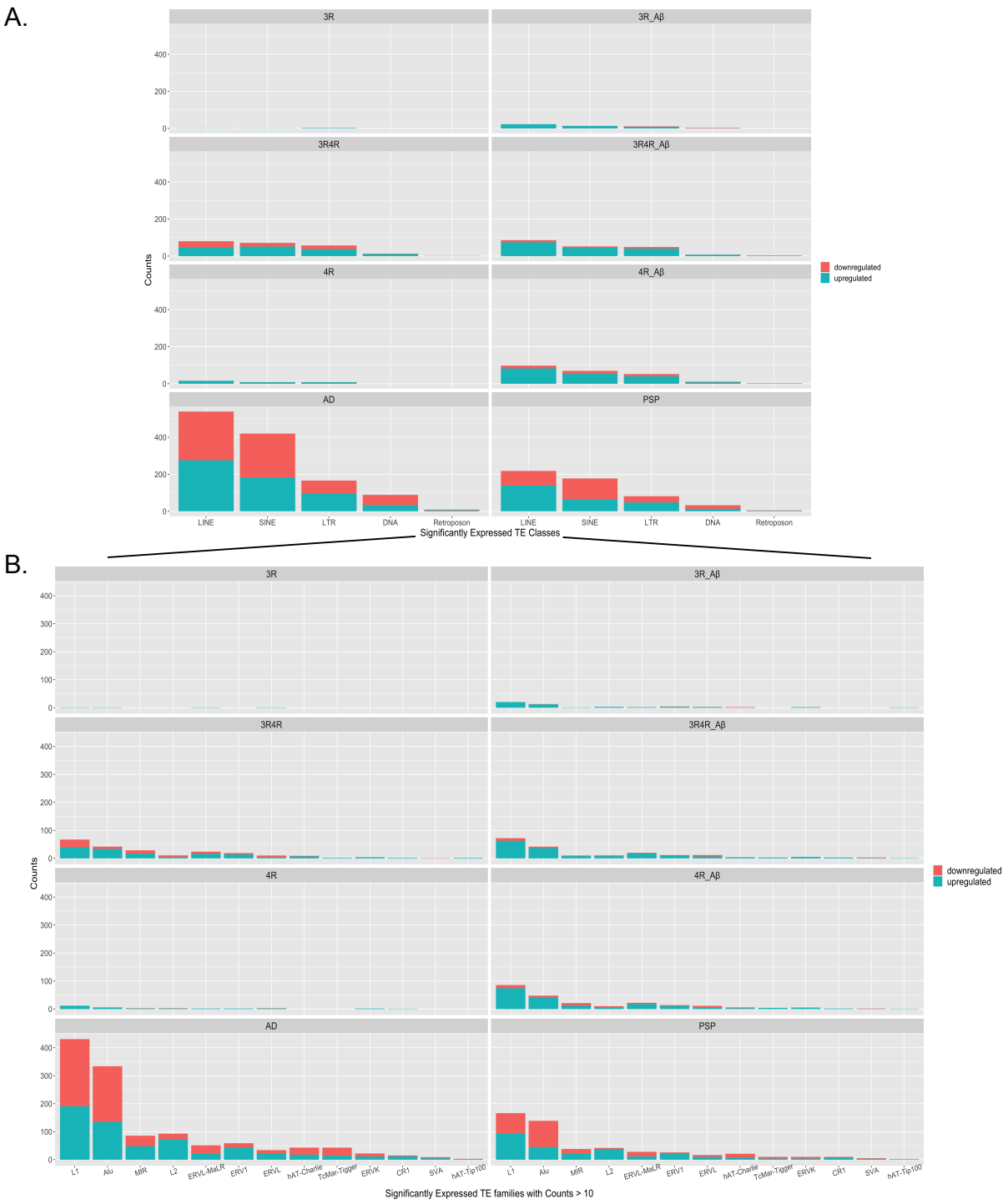

Figure 7. Classification of significantly differentially expressed locus-specific transposable elements by transposable element class and family. A. Counts of how many significantly differentially expressed TE loci there are (downregulated and upregulated) per condition grouped by class of TE. **B.** Counts (of families with counts > 10) of how many significantly differentially expressed TE loci there are (downregulated and upregulated) per condition grouped by TE family.

This thesis is currently being prepared for submission for publication of the material. Grundman, J., Spencer, B., Sarsoza, F., Rissman, R.A. The dissertation/thesis author was the primary investigator and author of this material.

References

Adams, S. J., de Ture, M. A., McBride, M., Dickson, D. W., & Petrucelli, L. (2010). Three repeat isoforms of tau inhibit assembly of four repeat tau filaments. PLoS ONE, 5(5). https://doi.org/10.1371/journal.pone.0010810

Allen, M., Carrasquillo, M. M., Funk, C., Heavner, B. D., Zou, F., Younkin, C. S., Burgess, J. D., Chai, H. S., Crook, J., Eddy, J. A., Li, H., Logsdon, B., Peters, M. A., Dang, K. K., Wang, X., Serie, D., Wang, C., Nguyen, T., Lincoln, S., Malphrus, K., … Ertekin-Taner, N. (2016). Human whole genome genotype and transcriptome data for Alzheimer's and other neurodegenerative diseases. Scientific data, 3, 160089. https://doi.org/10.1038/sdata.2016.89

Andrews, S. (2010). FastQC: A Quality Control Tool for High Throughput Sequence Data [Online]. Available online at: http://www.bioinformatics.babraham.ac.uk/projects/fastqc/

Dobin, A., Davis, C. A., Schlesinger, F., Drenkow, J., Zaleski, C., Jha, S., Batut, P., Chaisson, M., & Gingeras, T. R. (2013). STAR: ultrafast universal RNA-seq aligner. Bioinformatics (Oxford, England), 29(1), 15–21. https://doi.org/10.1093/bioinformatics/bts635

Forner, S., Baglietto-Vargas, D., Martini, A. C., Trujillo-Estrada, L., & LaFerla, F. M. (2017). Synaptic Impairment in Alzheimer's Disease: A Dysregulated Symphony. Trends in neurosciences, 40(6), 347–357. https://doi.org/10.1016/j.tins.2017.04.002

Frost, B., Bardai, F. H., & Feany, M. B. (2016). Lamin Dysfunction Mediates Neurodegeneration in Tauopathies. Current biology : CB, 26(1), 129–136. https://doi.org/10.1016/j.cub.2015.11.039

Frost, B., Hemberg, M., Lewis, J., & Feany, M. B. (2014). Tau promotes neurodegeneration through global chromatin relaxation. Nature neuroscience, 17(3), 357–366. https://doi.org/10.1038/nn.3639

Guo, C., Jeong, H. H., Hsieh, Y. C., Klein, H. U., Bennett, D. A., De Jager, P. L., Liu, Z., & Shulman, J. M. (2018). Tau Activates Transposable Elements in Alzheimer's Disease. Cell reports, 23(10), 2874–2880. https://doi.org/10.1016/j.celrep.2018.05.004

Guo, T., Noble, W., & Hanger, D. P. (2017). Roles of tau protein in health and disease. Acta neuropathologica, 133(5), 665–704. https://doi.org/10.1007/s00401-017-1707-9

Jin Y., Hammell M. (2018) Analysis of RNA-Seq Data Using TEtranscripts. In: Wang Y., Sun M. (eds) Transcriptome Data Analysis. Methods in Molecular Biology, vol 1751. Humana Press, New York, NY

Jin, Y., Tam, O. H., Paniagua, E., & Hammell, M. (2015). TEtranscripts: a package for including transposable elements in differential expression analysis of RNA-seq datasets. Bioinformatics (Oxford, England), 31(22), 3593–3599. https://doi.org/10.1093/bioinformatics/btv422

Kim, C., Rockenstein, E., Spencer, B., Kim, H., Adame, A., Trejo, M., Staga, K., Lee, H., Lee, S., Masliah, E. (2015). Antagonizing Neuronal Toll-like Receptor 2 Prevents Synucleinopathy by Activating Autophagy. Cell Rep 13(4): 771-782.

Klein, H. U., McCabe, C., Gjoneska, E., Sullivan, S. E., Kaskow, B. J., Tang, A., Smith, R. V., Xu, J., Pfenning, A. R., Bernstein, B. E., Meissner, A., Schneider, J. A., Mostafavi, S., Tsai, L. H., Young-Pearse, T. L., Bennett, D. A., & De Jager, P. L. (2019). Epigenome-wide study uncovers large-scale changes in histone acetylation driven by tau pathology in aging and Alzheimer's human brains. Nature Neuroscience, 22(1), 37–46. https://doi.org/10.1038/s41593-018-0291-1

Klein, S. J., & O'Neill, R. J. (2018). Transposable elements: genome innovation, chromosome diversity, and centromere conflict. Chromosome Research, 26(1–2), 5–23. https://doi.org/10.1007/s10577-017-9569-5

Lacovich, V., Espindola, S. L., Alloatti, M., Devoto, V. P., Cromberg, L. E., Čarna, M. E., Forte, G., Gallo, J. M., Bruno, L., Stokin, X. B., Avale, M. E., & Falzone, T. L. (2017). Tau isoforms imbalance impairs the axonal transport of the amyloid precursor protein in human neurons. Journal of Neuroscience, 37(1), 58–69. https://doi.org/10.1523/JNEUROSCI.2305-16.2016

Lebouvier, T., Pasquier, F., & Buée, L. (2017). Update on tauopathies. Current Opinion in Neurology, 30(6), 589–598. https://doi.org/10.1097/WCO.0000000000000502

Maina, M. B., Bailey, L. J., Doherty, A. J., & Serpell, L. C. (2018). The Involvement of Aβ42 and Tau in Nucleolar and Protein Synthesis Machinery Dysfunction. Frontiers in Cellular Neuroscience, 12(August), 1–13. https://doi.org/10.3389/fncel.2018.00220

Liao, Y., Smyth, G. K., & Shi, W. (2014). featureCounts: an efficient general purpose program for assigning sequence reads to genomic features. Bioinformatics (Oxford, England), 30(7), 923–930. https://doi.org/10.1093/bioinformatics/btt656

Love, M. I., Huber, W., & Anders, S. (2014). Moderated estimation of fold change and dispersion for RNA-seq data with DESeq2. *Genome biology*, *15*(12), 550. https://doi.org/10.1186/s13059-014-0550-8

Mansuroglu, Z., Benhelli-Mokrani, H., Marcato, V., Sultan, A., Violet, M., Chauderlier, A., Delattre, L., Loyens, A., Talahari, S., Bégard, S., Nesslany, F., Colin, M., Souès, S., Lefebvre, B., Buée, L., Galas, M. C., & Bonnefoy, E. (2016). Loss of Tau protein affects the structure, transcription and repair of neuronal pericentromeric heterochromatin. Scientific reports, 6, 33047. https://doi.org/10.1038/srep33047

Meier, S., Bell, M., Lyons, D. N., Rodriguez-Rivera, J., Ingram, A., Fontaine, S. N., Mechas, E., Chen, J., Wolozin, B., LeVine, H., 3rd, Zhu, H., & Abisambra, J. F. (2016). Pathological Tau Promotes Neuronal Damage by Impairing Ribosomal Function and Decreasing Protein Synthesis. The Journal of neuroscience : the official journal of the Society for Neuroscience, 36(3), 1001–1007. https://doi.org/10.1523/JNEUROSCI.3029-15.2016

Monroy-Ramirez, H. C., & Binder, L. I. (2013). Alterations in the Nuclear Architecture Produced by the Overexpression of Tau Protein in Neuroblastoma Cells. 36, 503–520. https://doi.org/10.3233/JAD-122401

Munoz-Lopez, M., & Garcia-Perez, J. (2010). DNA Transposons: Nature and Applications in Genomics. Current Genomics, 11(2), 115–128. https://doi.org/10.2174/138920210790886871

Moreira PI, Carvalho C, Zhu X, Smith MA, Perry G. Mitochondrial dysfunction is a trigger of Alzheimer's disease pathophysiology. Biochim Biophys Acta. 2010;1802(1):2-10. doi:10.1016/j.bbadis.2009.10.006

Okonechnikov, K., Conesa, A., & García-Alcalde, F. (2016). Qualimap 2: advanced multi-sample quality control for high-throughput sequencing data. Bioinformatics (Oxford, England), 32(2), 292–294. https://doi.org/10.1093/bioinformatics/btv566

O'Neill, K., Brocks, D., & Hammell, M. G. (2020). Mobile genomics: tools and techniques for tackling transposons. *Philosophical transactions of the Royal Society of London. Series B, Biological sciences*, *375*(1795), 20190345. https://doi.org/10.1098/rstb.2019.0345

Payer, L. M., & Burns, K. H. (2019). Transposable elements in human genetic disease. Nature Reviews Genetics, 20 (December), 760–772. https://doi.org/10.1038/s41576-019-0165-8

Rockenstein, E., Overk, C. R., Ubhi, K., Mante, M., Patrick, C., Adame, A., Bisquert, A., Trejo-Morales, M., Spencer, B., & Masliah, E. (2015). A novel triple repeat mutant tau transgenic model that mimics aspects of pick's disease and fronto-temporal tauopathies. PloS one, 10(3), e0121570. https://doi.org/10.1371/journal.pone.0121570

Sealey, M. A., Vourkou, E., Cowan, C. M., Bossing, T., Quraishe, S., Grammenoudi, S., Skoulakis, E., & Mudher, A. (2017). Distinct phenotypes of three-repeat and four-repeat human tau in a transgenic model of tauopathy. Neurobiology of disease, 105, 74–83. https://doi.org/10.1016/j.nbd.2017.05.003

Shanbhag, N. M., Evans, M. D., Mao, W., Nana, A. L., Seeley, W. W., Adame, A., Rissman, R. A., Masliah, E., & Mucke, L. (2019). Early neuronal accumulation of DNA

double strand breaks in Alzheimer's disease. Acta neuropathologica communications, 7(1), 77. https://doi.org/10.1186/s40478-019-0723-5

Sotiropoulos, I., Galas, M. C., Silva, J. M., Skoulakis, E., Wegmann, S., Maina, M. B., Blum, D., Sayas, C. L., Mandelkow, E. M., Mandelkow, E., Spillantini, M. G., Sousa, N., Avila, J., Medina, M., Mudher, A., & Buee, L. (2017). Atypical, non-standard functions of the microtubule associated Tau protein. Acta neuropathologica communications, 5(1), 91. https://doi.org/10.1186/s40478-017-0489-6

Spencer, B., Michael, S., Shen, J., Kosberg, K., Rockenstein, E., Patrick, C., Adame, A., & Masliah, E. (2013). Lentivirus mediated delivery of neurosin promotes clearance of wild-type α-synuclein and reduces the pathology in an α-synuclein model of LBD. Molecular therapy : the journal of the American Society of Gene Therapy, 21(1), 31–41. https://doi.org/10.1038/mt.2012.66

Stine, W. B., Jungbauer, L., Yu, C., & LaDu, M. J. (2011). Preparing synthetic Aβ in different aggregation states. Methods in molecular biology (Clifton, N.J.), 670, 13–32. https://doi.org/10.1007/978-1-60761-744-0_2

Sultan, A., Nesslany, F., Violet, M., Bégard, S., Loyens, A., Talahari, S., Mansuroglu, Z., Marzin, D., Sergeant, N., Humez, S., Colin, M., Bonnefoy, E., Buée, L., & Galas, M. C. (2011). Nuclear Tau, a key player in neuronal DNA protection. Journal of Biological Chemistry, 286(6), 4566–4575. https://doi.org/10.1074/jbc.M110.199976

Sun, W., Samimi, H., Gamez, M., Zare, H., & Frost, B. (2018). Pathogenic tau-induced piRNA depletion promotes neuronal death through transposable element dysregulation in neurodegenerative tauopathies. Nature Neuroscience, 21(8), 1038–1048. https://doi.org/10.1038/s41593-018-0194-1

Tam, O. H., Ostrow, L. W., & Gale Hammell, M. (2019). Diseases of the nERVous system: Retrotransposon activity in neurodegenerative disease. Mobile DNA, 10(1), 1–14. https://doi.org/10.1186/s13100-019-0176-1

Terry, D. M., & Devine, S. E. (2020). Aberrantly High Levels of Somatic LINE-1 Expression and Retrotransposition in Human Neurological Disorders. Frontiers in genetics, 10, 1244. https://doi.org/10.3389/fgene.2019.01244

Tiscornia, G., et al. (2006). Production and purification of lentiviral vectors. Nat Protoc 1(1):
241-245.

Violet, M., Delattre, L., Tardivel, M., Sultan, A., Chauderlier, A., Caillierez, R., Talahari, S., Nesslany, F., Lefebvre, B., Bonnefoy, E., Buée, L., & Galas, M.-C. (2014). A major role for Tau in neuronal DNA and RNA protection in vivo under physiological and hyperthermic conditions. Frontiers in Cellular Neuroscience, 8(March), 1–11. https://doi.org/10.3389/fncel.2014.00084

Xicoy, H., Wieringa, B., & Martens, G. J. (2017). The SH-SY5Y cell line in Parkinson's disease research: a systematic review. Molecular neurodegeneration, 12(1), 10. https://doi.org/10.1186/s13024-017-0149-0

Yu, G., Wang, L. G., Han, Y., & He, Q. Y. (2012). clusterProfiler: an R package for comparing biological themes among gene clusters. Omics : a journal of integrative biology, 16(5), 284–287. https://doi.org/10.1089/omi.2011.0118

Zempel, H., Thies, E., Mandelkow, E., & Mandelkow, E. M. (2010). Abeta oligomers cause localized Ca(2+) elevation, missorting of endogenous Tau into dendrites, Tau phosphorylation, and destruction of microtubules and spines. The Journal of neuroscience : the official journal of the Society for Neuroscience, 30(36), 11938–11950. https://doi.org/10.1523/JNEUROSCI.2357-10.2010